

Local porosity measurement from scanning electron microscopy images in backscattered
electrons mode

Supplementary materials

Loïc Sorbier, Hedwige Poncet, Vincent Lecocq, Guillaume Maillet, Maroua Moula, Vincent Le

Corre

IFP Energies nouvelles, Rond-point de l'échangeur de Solaize, BP 3, 69360 Solaize, France

Corresponding author : Loïc Sorbier, Tel : (+33) 4 37 70 29 69, Fax : (+33) 4 37 70 27 45,

loic.sorbier@ifpen.fr

Uncertainty in ε

The porosity ε reads:

$$\varepsilon = \frac{\mathcal{V}_r Z_b^x (\eta_b - \bar{\eta})}{\mathcal{V}_r Z_b^x (\eta_b - \bar{\eta}) + \mathcal{V}_b Z_r^x (\bar{\eta} - \eta_r)} \quad (1)$$

Let x_i , $i \in \{1, \dots, N\}$, be N statically independent variables with uncertainties u_{x_i} . Let $f(x_i)$ be a moderately non-linear function of the variable x_i . If the u_{x_i} are small then u_f the uncertainty in $f(x_i)$ reads:

$$u_f^2 \approx \sum_{i=1}^N \left| \frac{\partial f}{\partial x_i} \right|^2 u_{x_i}^2 \quad (2)$$

From equation (1) we obtain:

$$\frac{\partial \varepsilon}{\partial \mathcal{V}_r} = \frac{\mathcal{V}_b Z_b^x Z_r^x (\eta_b - \bar{\eta})(\bar{\eta} - \eta_r)}{[\mathcal{V}_r Z_b^x (\eta_b - \bar{\eta}) + \mathcal{V}_b Z_r^x (\bar{\eta} - \eta_r)]^2} = \varepsilon^2 \frac{\mathcal{V}_b Z_r^x \bar{\eta} - \eta_r}{\mathcal{V}_r^2 Z_b^x \eta_b - \bar{\eta}} \quad (3)$$

$$\frac{\partial \varepsilon}{\partial \mathcal{V}_b} = \frac{-\mathcal{V}_r Z_b^x Z_r^x (\eta_b - \bar{\eta})(\bar{\eta} - \eta_r)}{[\mathcal{V}_r Z_b^x (\eta_b - \bar{\eta}) + \mathcal{V}_b Z_r^x (\bar{\eta} - \eta_r)]^2} = -\varepsilon^2 \frac{Z_r^x \bar{\eta} - \eta_r}{\mathcal{V}_r Z_b^x \eta_b - \bar{\eta}} \quad (4)$$

$$\frac{\partial \varepsilon}{\partial Z_r^x} = \frac{-\mathcal{V}_b \mathcal{V}_r Z_b^x (\eta_b - \bar{\eta})(\bar{\eta} - \eta_r)}{[\mathcal{V}_r Z_b^x (\eta_b - \bar{\eta}) + \mathcal{V}_b Z_r^x (\bar{\eta} - \eta_r)]^2} = -\varepsilon^2 \frac{\mathcal{V}_b \bar{\eta} - \eta_r}{\mathcal{V}_r Z_b^x \eta_b - \bar{\eta}} \quad (5)$$

$$\frac{\partial \varepsilon}{\partial Z_b^x} = \frac{\mathcal{V}_b \mathcal{V}_r Z_r^x (\eta_b - \bar{\eta})(\bar{\eta} - \eta_r)}{[\mathcal{V}_r Z_b^x (\eta_b - \bar{\eta}) + \mathcal{V}_b Z_r^x (\bar{\eta} - \eta_r)]^2} = \varepsilon^2 \frac{\mathcal{V}_b Z_r^x \bar{\eta} - \eta_r}{\mathcal{V}_r Z_b^{x^2} \eta_b - \bar{\eta}} \quad (6)$$

$$\frac{\partial \varepsilon}{\partial \eta_b} = \frac{\mathcal{V}_b \mathcal{V}_r Z_b^x Z_r^x (\bar{\eta} - \eta_r)}{[\mathcal{V}_r Z_b^x (\eta_b - \bar{\eta}) + \mathcal{V}_b Z_r^x (\bar{\eta} - \eta_r)]^2} = \varepsilon^2 \frac{\mathcal{V}_b Z_r^x \bar{\eta} - \eta_r}{\mathcal{V}_r Z_b^x (\eta_b - \bar{\eta})^2} \quad (7)$$

$$\frac{\partial \varepsilon}{\partial \eta_r} = \frac{\mathcal{V}_b \mathcal{V}_r Z_b^x Z_r^x (\eta_b - \bar{\eta})}{[\mathcal{V}_r Z_b^x (\eta_b - \bar{\eta}) + \mathcal{V}_b Z_r^x (\bar{\eta} - \eta_r)]^2} = \varepsilon^2 \frac{\mathcal{V}_b Z_r^x}{\mathcal{V}_r Z_b^x \eta_b - \bar{\eta}} \quad (8)$$

$$\frac{\partial \varepsilon}{\partial \bar{\eta}} = \frac{-\mathcal{V}_b \mathcal{V}_r Z_b^x Z_r^x (\eta_b - \eta_r)}{[\mathcal{V}_r Z_b^x (\eta_b - \bar{\eta}) + \mathcal{V}_b Z_r^x (\bar{\eta} - \eta_r)]^2} = -\varepsilon^2 \frac{\mathcal{V}_b Z_r^x \eta_b - \eta_r}{\mathcal{V}_r Z_b^x (\eta_b - \bar{\eta})^2} \quad (9)$$

From which we recover equation (9) of the paper :

$$\frac{u_\varepsilon^2}{\varepsilon^2} \approx \varepsilon^2 \left(\frac{\mathcal{V}_b Z_r^x}{\mathcal{V}_r Z_b^x} \right)^2 \times \left[\left(\frac{\bar{\eta} - \eta_r}{\eta_b - \bar{\eta}} \right)^2 \left(\frac{u_{\mathcal{V}_b^2}}{\mathcal{V}_b^2} + \frac{u_{\mathcal{V}_r^2}}{\mathcal{V}_r^2} + \frac{u_{Z_b^{x^2}}}{Z_b^{x^2}} + \frac{u_{Z_r^{x^2}}}{Z_r^{x^2}} \right) + \frac{1}{(\eta_b - \bar{\eta})^4} \right] \left[[(\bar{\eta} - \eta_r)^2 u_{\eta_b^2} + (\eta_b - \bar{\eta})^2 u_{\eta_r^2} + (\eta_b - \eta_r)^2 u_{\bar{\eta}^2}] \right] \quad (10)$$

Equation (10) is undefined for $\bar{\eta} = \eta_b$ ($\varepsilon = 0$) so that uncertainty must be obtained by another way. Let $f = 1 - \varepsilon$ be the volume fraction of matter. Obviously we have $u_\varepsilon = u_f$ and:

$$f = \frac{\mathcal{V}_b Z_r^x (\bar{\eta} - \eta_r)}{\mathcal{V}_r Z_b^x (\eta_b - \bar{\eta}) + \mathcal{V}_b Z_r^x (\bar{\eta} - \eta_r)} \quad (11)$$

The same procedure of uncertainty propagation leads to:

$$\frac{u_f^2}{f^2} \approx f^2 \left(\frac{\mathcal{V}_r Z_b^x}{\mathcal{V}_b Z_r^x} \right)^2 \times \left[\left(\frac{\eta_b - \bar{\eta}}{\bar{\eta} - \eta_r} \right)^2 \left(\frac{u_{\mathcal{V}_b^2}}{\mathcal{V}_b^2} + \frac{u_{\mathcal{V}_r^2}}{\mathcal{V}_r^2} + \frac{u_{Z_b^{x^2}}}{Z_b^{x^2}} + \frac{u_{Z_r^{x^2}}}{Z_r^{x^2}} \right) + \frac{1}{(\bar{\eta} - \eta_r)^4} \right] \left[[(\bar{\eta} - \eta_r)^2 u_{\eta_b^2} + (\eta_b - \bar{\eta})^2 u_{\eta_r^2} + (\eta_b - \eta_r)^2 u_{\bar{\eta}^2}] \right] \quad (12)$$

Equation (12) allows to evaluate the uncertainty in ε close to $\varepsilon = 0$. It is not defined for $\bar{\eta} = \eta_r$ ($\varepsilon = 1$).

Uncertainty in $\bar{\eta}$

Let $E[\]$ be the expectation and $\text{Var}[\]$ the variance. Figure 1 presents the detection chain for the acquisition of backscattered electron signal on a single pixel (see (Reimer 2010) p196). During the detection time, a number n_p of impinging electron is set on the sample. n_p follow a Poisson distribution with $\text{Var}[n_p] = E[n_p] = N$. A fraction of this incoming electrons $E[n_d] = \text{Var}[n_d] = \bar{\eta}N$ enter the detector and are converted into a signal x with $E[n_d] = G\bar{\eta}N$. The variance of x reads :

$$\text{Var}[x] = G^2 \text{Var}[n_d] + E_p^2 = G^2 E[n_d] + E_p^2 \quad (13)$$

Where E_p is an electronic noise independent of the number of detected electrons.

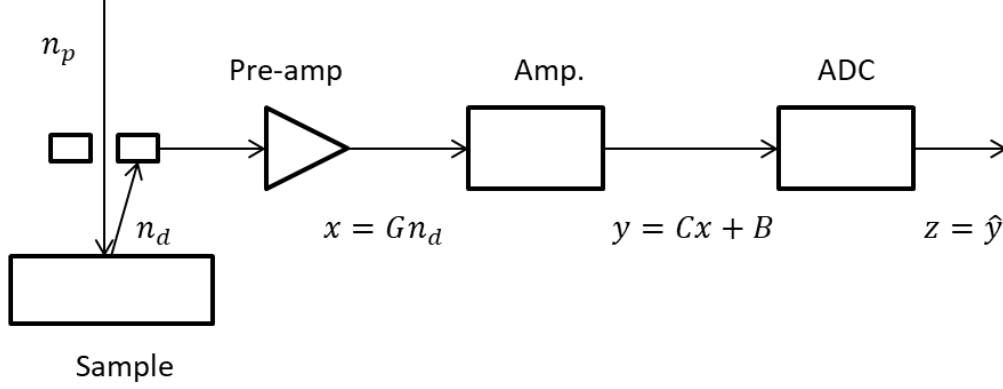


Figure 1 : Scheme of the detection chain. Pre-amp.: pre amplifier; Amp.: amplifier; ADC: analog to digital converter.

The signal $y = Cx + B$ coming out the amplifier is submitted to an electronic noise E_a independent of x so that :

$$\text{Var}[y] = \text{Var}[Cx + B] = C^2 \text{Var}[x] = C^2 G^2 E[n_d] + C^2 E_p^2 + E_a^2 \quad (14)$$

The standard uncertainty u_y in the signal y reads:

$$u_y^2 = \text{Var}[y] = C^2 G^2 E[n_d] + C^2 E_p^2 + E_a^2 \quad (15)$$

The analog to digital converter adds another contribution to the digital signal \hat{y} so that its standard uncertainty $u_{\hat{y}}$ reads:

$$\begin{aligned} u_{\hat{y}}^2 &= u_y^2 + \frac{1}{12} \\ &= C^2 G^2 E[n_d] + C^2 E_p^2 + E_a^2 + \frac{1}{12} \\ &= CG\hat{y} - B + C^2 E_p^2 + E_a^2 + \frac{1}{12} \\ &= \alpha \hat{y} + \beta \end{aligned} \quad (16)$$

Optimal working distance

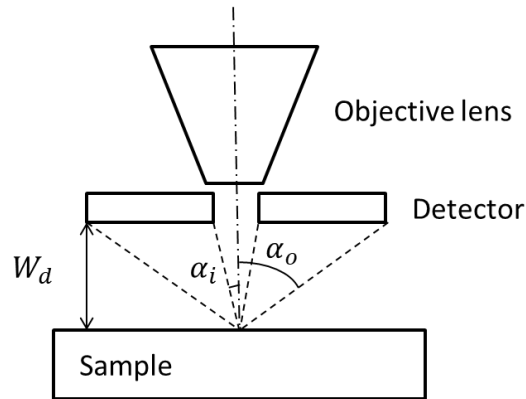


Figure 2 : Scheme of the detector geometry.

Figure 2 describes the geometry of the annular detector. The relations between the internal radius of the detector r_i , its external radius r_o , the working distance W_d and the collection angle range $[\alpha_i; \alpha_o]$ read:

$$\tan \alpha_i = \frac{r_i}{W_d} \quad (17)$$

$$\tan \alpha_o = \frac{r_o}{W_d} \quad (18)$$

The angular distribution of backscattered electrons is well approximated by a Lambert's law:

$$\frac{d\eta}{d\Omega} = \frac{\eta}{\pi} \cos \alpha \quad (19)$$

Hence the detected signal η_d may be approximated by :

$$\begin{aligned} \eta_d &= \frac{\eta}{\pi} \int_{\alpha_i}^{\alpha_o} \cos \alpha \, d\Omega \\ &= 2\eta \int_{\alpha_i}^{\alpha_o} \cos \alpha \sin \alpha \, d\alpha \\ &= \eta \int_{\alpha_i}^{\alpha_o} \sin 2\alpha \, d\alpha \\ &= \frac{\eta}{2} (\cos 2\alpha_i - \cos 2\alpha_o) \end{aligned} \quad (20)$$

Using the trigonometric identity $\cos 2\alpha = (1 - \tan^2 \alpha)/(1 + \tan^2 \alpha)$ in Equation (19) in combination with Equations (17) and (18) we obtain :

$$\eta_d = \frac{\eta}{2} \left(\frac{1 - \frac{r_i^2}{W_d^2}}{1 + \frac{r_i^2}{W_d^2}} - \frac{1 - \frac{r_o^2}{W_d^2}}{1 + \frac{r_o^2}{W_d^2}} \right) \quad (21)$$

$$= \frac{\eta W_d^2 (r_o^2 - r_i^2)}{(W_d^2 + r_i^2)(W_d^2 + r_o^2)}$$

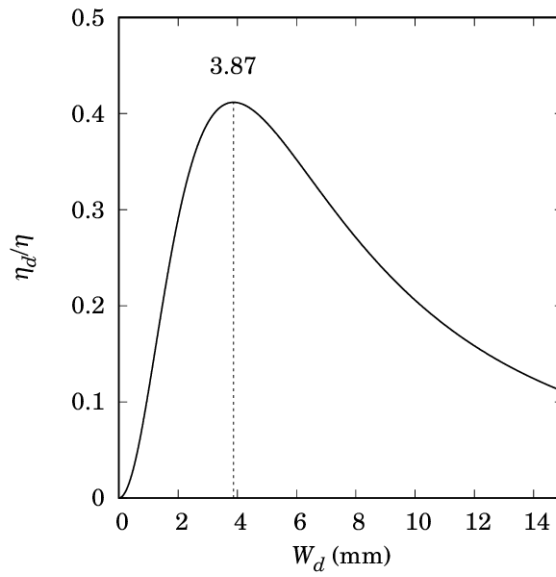


Figure 3 : Theoretical influence of the working distance on the detected signal for detector radii given by the microscope manufacturer $r_i = 2.5$ mm et $r_o = 6$ mm. Dotted line indicates the optimal working distance \widehat{W}_d .

Figure 3 shows the influence of the working distance on the detected signal with internal and external radii given by the microscope manufacturer. There exists an optimal working distance where the detected signal is the higher. Close to this maximum, the detected signal is very weakly dependent on the precise value of the working distance. From Equation (21) we obtain:

$$\frac{\partial \eta_d}{\partial W_d} = \frac{2\eta W_d (r_i^2 r_o^2 - W_d^4)}{(W_d^2 + r_i^2)^2 (W_d^2 + r_o^2)^2} \quad (22)$$

Then the optimal working distance \widehat{W}_d is obtained when $\frac{\partial \eta_d}{\partial W_d}(\widehat{W}_d) = 0$:

$$\widehat{W}_d = \sqrt{r_i r_o} \quad (23)$$

Thus a small variation of 0.3 mm around $\widehat{W}_d \approx 3.87$ mm leads to a variation of signal less than 0.6 %.

If experimental backscattering signal \hat{y} is concerned Equation (21) has to be corrected with the contrast (α) and brightness (β) ajustements and with a deviation of the indicated working distance given by the microscope (W_d) from the true working distance ($W_d - \delta$).

Then Equation (21) transforms into:

$$\hat{y} = \alpha \frac{\eta (W_d - \delta)^2 (r_o^2 - r_i^2)}{((W_d - \delta)^2 + r_i^2)((W_d - \delta)^2 + r_o^2)} + \beta \quad (24)$$

Hence optimal indicated working distance is given by $\widehat{W}_d = \sqrt{r_i r_o} + \delta$. Figure 4 shows the mean grey levels measured on a same zone containing resin and massive alumina with the same adjustments for contrast and brightness but with varying the working distance. The continuous curves are a simultaneous least square fit of Equation (24) on both resin and alumina with only α , β and δ as free parameters. Values of $r_i = 2.5$ mm and $r_o = 6$ mm are given by the microscope manufacturer. The value for η for resin and alumina is taken from the Monte-Carlo simulations. The agreement between data and theoretical model of Equation (23) is very satisfactory. A very poor fit is obtained if the parameter δ is omitted.

Optimized values of the parameters are given in Table 1. The value obtained for δ (406 μ m) is not surprising taking into account the practical difficulty to precisely calibrate the working distance on a SEM. The discrepancies between data and model shown on the three lowest

working distance for resin are due to the damage done to the resin after seven frames acquisition.

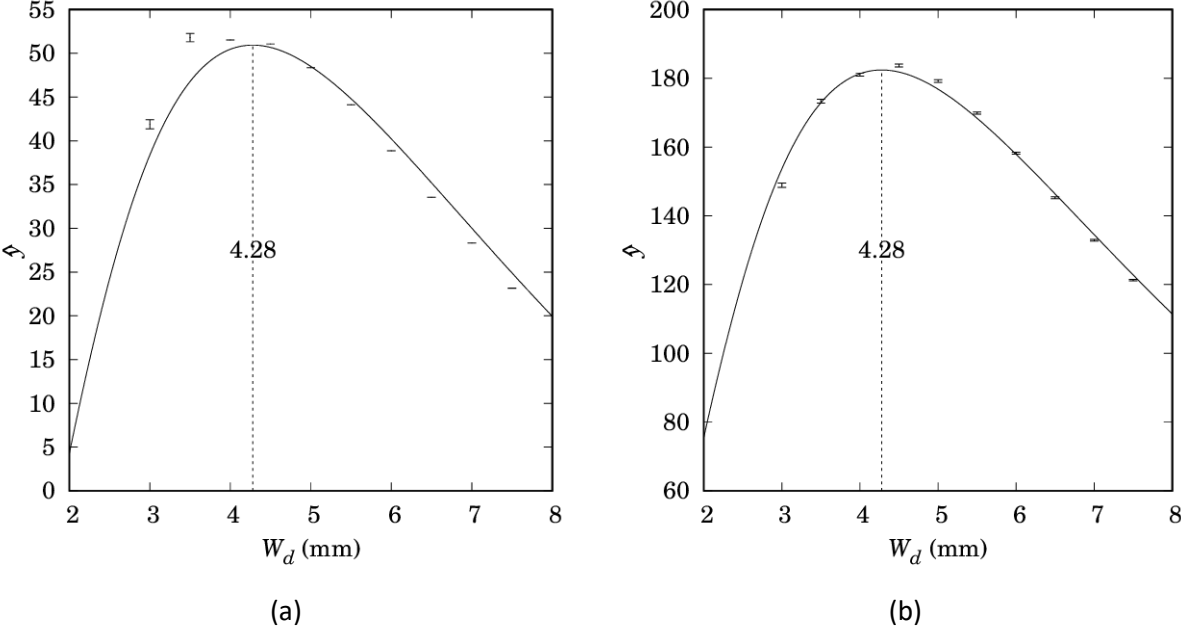


Figure 4 : Mean grey levels \hat{y} on (a) PMMA resin and (b) massive alumina as function of the indicated working distance W_d . Symbols are experimental data and continuous lines are the results of the least square fit of Equation (24).

Table 1: Optimized parameters for least square fit of Equation (23) shown in Figure (4)

Parameter	Value
α	4134
β	-50.94
δ (mm)	0.4058

High resolution SEM images

A section of impregnated extrudates of sample B3000 was milled and thin slices were cut at a 300 nm thickness by a RMC PowerTome PT PCZ ultramicrotome fitted with a diamond knife. Thin sections were deposited on an aluminum stub and observed with a FEI Nova NanoSEM in low vacuum mode (10 Pa H₂O) at 5 kV with a GAD detector.

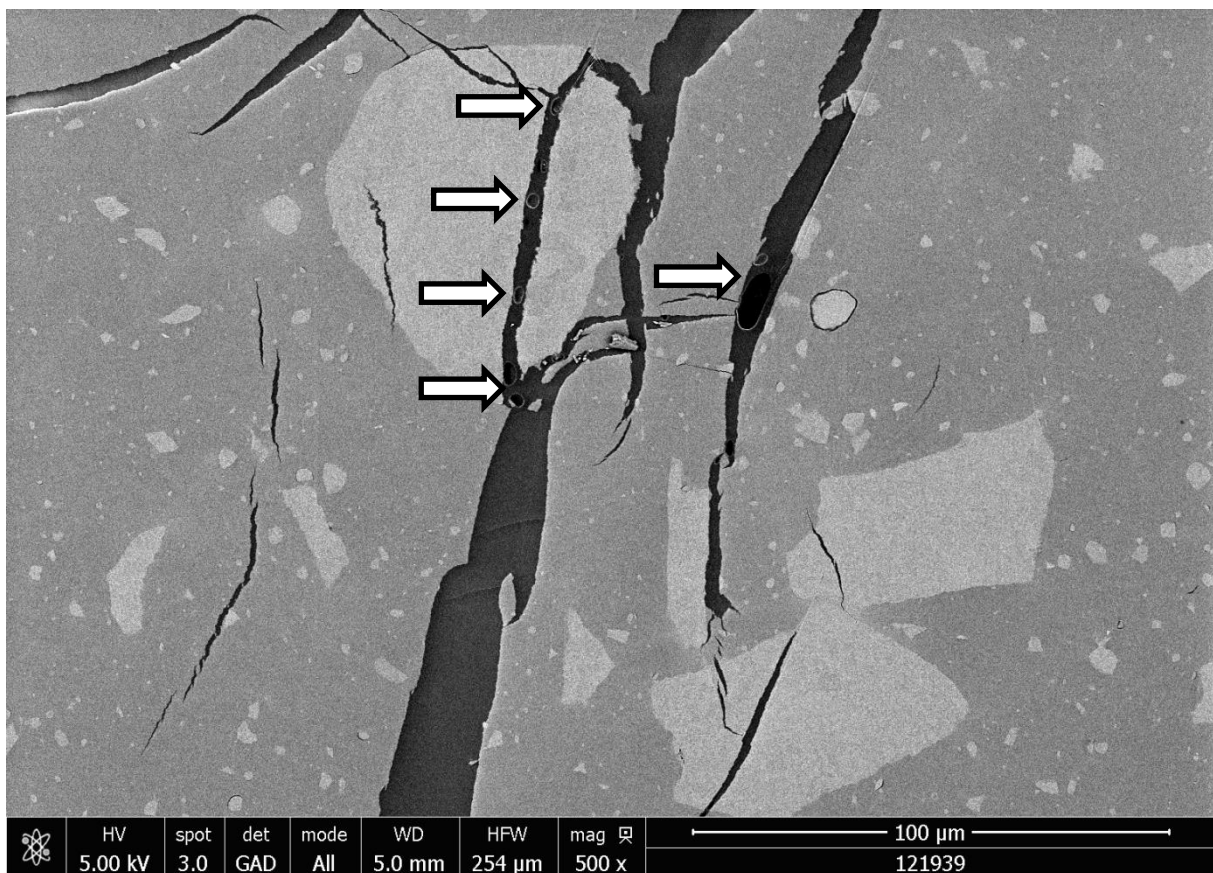


Figure 5 : Low resolution SEM image of thin slice of sample B3000 showing rare cavities (arrows) due to porosity not impregnated with resin.

Figure 5 shows a low resolution SEM image of a rare part of the B3000 where cracks are observed. Bubbles due to improper resin impregnation are sometimes observed in these cracks. Figure 6 is a high resolution SEM image of the same sample. No evidence of unfilled pores are observed.

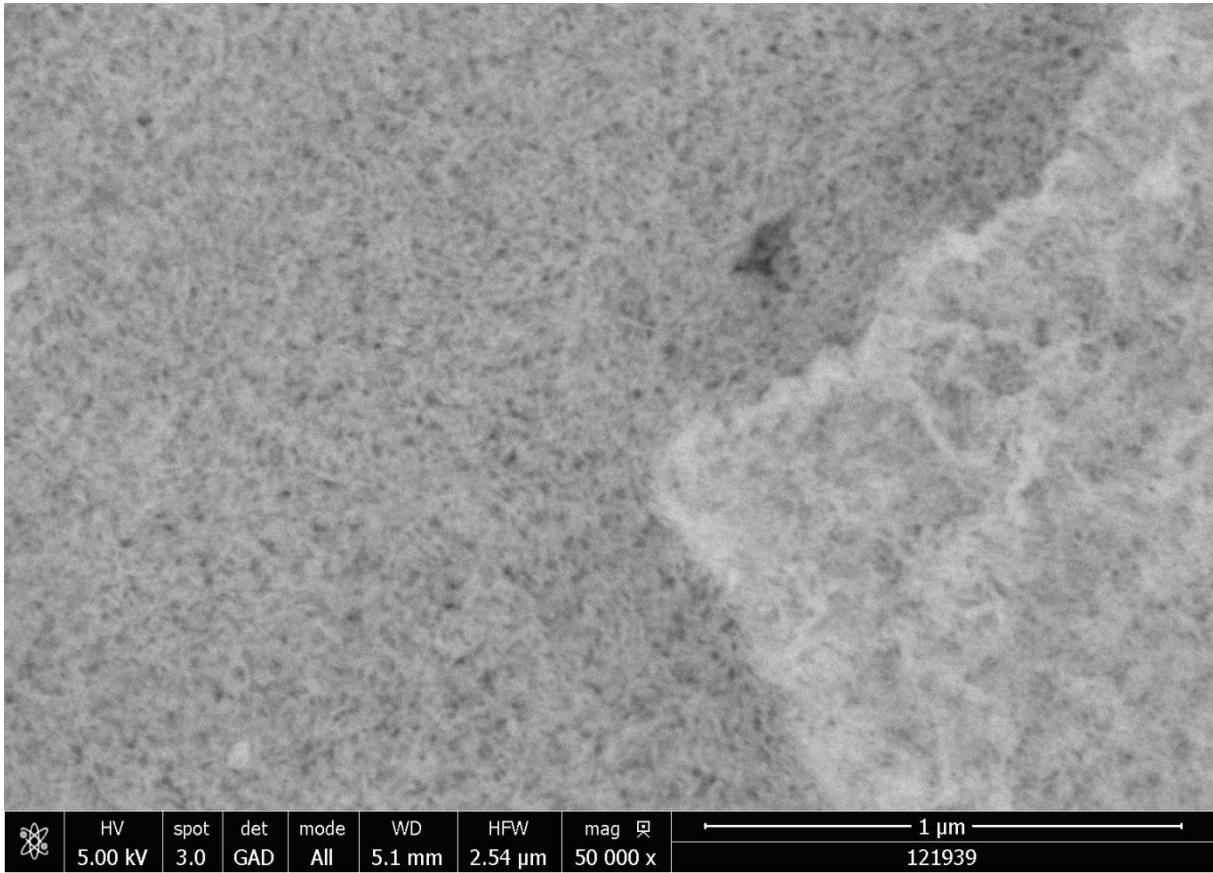


Figure 6 : High resolution SEM image of thin slice of sample B3000 showing no cavities due to porosity not impregnated with resin.

References

Reimer, L. 2010. Scanning electron microscopy: Physics of image formation and microanalysis, Second revised and updated edition. Heidelberg: Springer.